

RESEARCH ARTICLE | FEBRUARY 17 2010

## Phononic gaps in thin semiconductor superlattices

S. P. Hepplestone; G. P. Srivastava



*J. Appl. Phys.* 107, 043504 (2010)

<https://doi.org/10.1063/1.3285415>



### Articles You May Be Interested In

Impact of interfacial thickness on Raman intensity profiles and phonon anisotropy in short-period  $(\text{AlSb})_n/(\text{GaSb})_m$  superlattices

*J. Vac. Sci. Technol. A* (July 2022)

Superlatticed negative differential-resistance heterojunction bipolar transistor

*J. Vac. Sci. Technol. B* (July 1999)

Observation of the impulse-like negative-differential resistance of superlatticed resonant-tunneling transistor

*Appl. Phys. Lett.* (July 1999)



Journal of Applied Physics

## Special Topics Open for Submissions

[Learn More](#)

# Phononic gaps in thin semiconductor superlattices

S. P. Hepplestone<sup>a)</sup> and G. P. Srivastava*School of Physics, University of Exeter, Stocker Road, Exeter EX4 4QL, United Kingdom*

(Received 18 November 2009; accepted 30 November 2009; published online 17 February 2010)

We have studied one-dimensional phononic gaps in thin semiconductor superlattices. A general methodology has been developed for predicting the locations of these gaps in both thin and thick superlattices. Quantitative analysis of results for the phonon dispersions of Si/Ge[001] and GaAs/AlAs[001] superlattices are presented as both a function of period and composition. The effect of interface mixing is studied and its effects are found to be smaller than previously guessed. The introduction of the defects is shown to not change the phononic gap characteristics significantly. Finally, we present a discussion on the merits and uses of one-dimensional phononic structures.

© 2010 American Institute of Physics. [doi:[10.1063/1.3285415](https://doi.org/10.1063/1.3285415)]

## I. INTRODUCTION

Nanophononics is an emerging field of research with great potential for enabling phonon engineering and hence manipulation of sound and heat at the nanoscale. Several groups have examined systems for which phonon frequency gaps exist either in one direction, two directions, or all three directions.<sup>1–8</sup> These structures present excellent opportunities to engineer systems with great anisotropy in their vibrational and phonon-related thermal properties. A group of potential nanophononic structures are superlattices.<sup>1,2,9</sup> Such solid/solid systems present challenges with regards to locating phononic gaps as the differing velocities of the transverse and longitudinal branches make predictions difficult. Also, these systems do not present a true “forbidden zone” as the directions perpendicular to the growth direction will not have gaps and may have phonon modes with components of the velocity in the direction of growth. These crystals have a large number of applications, including much improved thermoelectrics<sup>10</sup> and phonon filters.<sup>5</sup> In particular, the large difference in the thermal properties between the growth direction and the in-plane directions owes directly to the changes in phonon properties in the growth direction.

During the late 1980s and early 1990s superlattices (especially Si/Ge and GaAs/AlAs) were studied in some depth with several different methods being employed. Multiple techniques including *ab initio*,<sup>11,12</sup> phenomenological atomic models,<sup>13,14</sup> and most notably Rytov’s continuum model<sup>15</sup> were applied to model phonon dispersion curves in these systems. The main emphasis of these studies was to investigate the behavior of the confined optical modes and their dependence on material composition and period.<sup>16–18</sup> In recent years, the development and improvement of pump probe subpicosecond techniques<sup>19</sup> has enabled the examination of the acoustic region in considerable detail. In particular, this technique has allowed the determination of stop bands in specific directions within these structures. These stop bands are also referred to as one-dimensional phononic gaps. This has reinvigorated theoretical investigations of the phonon spectra in the acoustic range using a range of techniques. In

particular, an investigation of the behavior of these stop bands as a function of packing or length fraction and with period is of great importance, as is the effect of interface mixing and imperfect interfaces on this functionality. The vibrational properties of phononic structures have mostly been studied by employing the elastic continuum theory.<sup>15,19–23</sup> This theory is generally unable to produce the full vibrational spectrum and its application at the nanoscale becomes unphysical. These continuum models have several features which make them inapplicable to nanoscale phononic systems. First, they rely on several different parameters which are generally based upon apriori knowledge of the bulk phonon velocities and densities. These values change in nanoscale systems where the interface structure dominates the phonon properties. Also, these models cannot account for the splitting of the transverse acoustic branches in the [110] direction in bulk silicon without introducing more parameters.<sup>24–26</sup> At the atomic level, superlattices have been studied using atomic scale phenomenological models, but for phononic systems only a few ball-and-spring models<sup>27,28</sup> have been applied. However, atomic models are required to study the vibrational properties of nanophononic systems in full (i.e., covering the whole frequency range and all phonon polarisations), including examination of the interface regions in detail.

Recent experimental measurements using subpicosecond acoustics techniques have found the locations and widths of gaps in the longitudinal acoustic (LA) spectra in Si/SiGe[001] (Ref. 19) and GaAs/AlAs[001] (Ref. 29) superlattices, suggesting that these could be one-dimensional phononic crystals. However, not being able to measure the transverse acoustic (TA) spectra, these experiments were unable to ascertain if the systems were one-dimensional phononic crystals or not. In a recent theoretical work,<sup>30</sup> we have shown that the Si(4 nm)/Si<sub>0.4</sub>Ge<sub>0.6</sub>(8 nm)[001] superlattice fabricated by Ezzahri *et al.*<sup>19</sup> is indeed a one-dimensional phononic system, i.e., in the superlattice growth direction there is a common gap of 8 GHz centered around 510 GHz between the LA and TA branches. We also showed that varying the structural composition of the Si<sub>0.4</sub>Ge<sub>0.6</sub> layer leads to a relatively small shift in the frequencies.

<sup>a)</sup>Electronic mail: [hepple@excc.ex.ac.uk](mailto:hepple@excc.ex.ac.uk).

In this work, we have employed an enhanced version<sup>30</sup> of the adiabatic bond charge model<sup>31–34</sup> of lattice dynamics to study phononic gaps in thin semiconductor superlattices. From the results obtained for the full phonon spectrum, we present firm trends for phononic gaps dependent on superlattice composition and period. We also provide an effective methodology, via understanding the LA and TA gaps, of predicting the one-dimensional phononic behavior. From this information, we are able to not only predict results for larger one-dimensional phononic structures, but also comment on general features of phonon related thermal properties of solid/solid systems.

## II. METHODOLOGY

We applied an enhanced adiabatic bond charge model for calculating the phonon dispersion relations in several thin  $(A)_n(B)_m[001]$  superlattices, where  $n$  and  $m$  indicate the number of atomic bilayers of the constituent materials in the supercell. The enhanced adiabatic bond charge model<sup>30</sup> is similar to the original atomic-scale bond charge model proposed by Weber and Rustagi.<sup>31</sup> In this approach, the valence charge distribution in tetrahedrally bonded materials is represented as point charges, called bond charges. Consistent with the maximum in the electronic charge distribution, the bond charges are located midway between homopolar bonds and slightly toward the anion for heteropolar bonds. Furthermore, the bond charges are assumed to have zero mass and are allowed to move adiabatically. The equations of motion for the ions and the bond charges are evaluated and a dynamical matrix is obtained by considering three types of interaction: (i) Coulomb interaction between all particles within the structure, which is evaluated using the Ewald summation technique, (ii) short range central force interaction acting centrally between nearest neighbors, and (iii) a rotationally invariant Keating type bond bending interaction,<sup>35</sup> depending on the angle between the ions and the bond-charges. Such an approach requires four (six) parameters to model the phonon dispersion relations of IV-IV (III-V) bulk semiconductors. The parameters for the systems studied here are taken from previous works.<sup>31,32</sup>

The enhancement in the original adiabatic bond charge model for the calculation of the phonon dispersion relations of composite structures is accomplished by considering the required interaction parameters for bonds at a superlattice interface as appropriately weighted average values for the two constituent materials. This technique produces phonon dispersion results for  $\text{Si}_x\text{Ge}_{1-x}$  alloys in good agreement with Brya's measurements.<sup>36</sup> We have also shown<sup>30</sup> that the method produces phonon polarization gaps in the  $\text{Si}(4\text{ nm})/\text{Si}_{0.4}\text{Ge}_{0.6}(8\text{ nm})[001]$  superlattice in excellent agreement with subpicosecond measurements.<sup>19</sup> It is important to note that while strain effects may lead to changes in the bond strength at interfaces, as  $\omega \propto \sqrt{\alpha}$ , where  $\alpha$  is the force constant, the overall effect is not expected to be significant, especially as modeled parameters provide results which agree with experimental values. A further validation of this technique is established by noting very good agreement between our results and previously understood trends for the

TABLE I. The cubic lattice constants and atomic masses for the bulk semiconductors used in this work. Note that the average mass is given purely for information and is not used within our atomic model.

Bulk material	Cubic lattice constant (nm)	Cation mass (amu)	Anion mass (amu)	Average atomic mass (amu)
Si	0.543	28.09	28.09	28.09
Ge	0.565	72.61	72.61	72.61
Sn	0.646	118.71	118.71	118.71
GaAs	0.565	69.72	74.92	72.32
AlAs	0.565	26.98	74.92	50.95
GaN	0.449	69.72	14.01	41.87
InN	0.438	114.82	14.01	64.42

highest optical phonon mode in superlattices of various periods.<sup>16,17</sup> The success of this model in explaining these and other results,<sup>32</sup> shows that this model can accurately be applied to examine phonon dispersion relations in nanoscale systems in which interface effects (both bonding and atomic mixing) play an important role.

For a superlattice  $(A)_n(B)_m$  grown along  $[001]$  we define the length fraction or percentage of material  $B$  as  $L_f = m/(n+m)$  and the superlattice period as  $L_0 = na_A/2 + ma_B/2$ , where  $a_A(a_B)$  is the cubic lattice constant of material  $A(B)$ . Two bilayers of a material is equivalent in size to one cubic lattice constant. For brevity, we will use the notation  $(n,m)$  for a  $(A)_n(B)_m$  superlattice. For ease of reference, the cubic lattice constants and atomic masses are listed in Table I.

## III. RESULTS AND DISCUSSION

### A. One-dimensional phononics

We have computed and analyzed the phonon dispersion relations for five thin semiconducting  $[001]$  superlattices:  $(\text{Si})_2(\text{Ge})_2$ ,  $(\text{Si})_2(\text{Sn})_2$ ,  $(\text{Ge})_2(\text{Sn})_2$ ,  $(\text{GaAs})_2(\text{AlAs})_2$ , and  $(\text{AlN})_2(\text{InN})_2$ . This selection of systems is expected to provide interesting and useful results which highlight the important features. Layers of  $\text{Si}/\text{Ge}$ ,<sup>1</sup>  $\text{GaAs}/\text{AlAs}$ ,<sup>2</sup>  $\text{Si}/\text{Sn}$ ,<sup>37</sup>  $\text{Ge}/\text{Sn}$ ,<sup>38</sup> and  $\text{AlN}/\text{InN}$  (Ref. 39) have successfully been grown using modern growth techniques, clearly suggesting that these structures are realizable in practice.

As can be seen from Fig. 1, gaps appear in the LA and TA acoustic phonon spectra in the growth direction for all the superlattices studied. We will denote these gaps as  $\text{LAN}$  and  $\text{TAN}$ , with  $n$  taking odd and even numbers for gaps at the zone edge and zone center, respectively. For each system we have highlighted in Fig. 1 the lowest transverse and longitudinal polarization gaps as  $\text{TA1}$  and  $\text{LA1}$ , respectively. For all the five systems the first longitudinal gap ( $\text{LA1}$ ) coincides with a gap in the transverse mode (higher than the  $\text{TA1}$  gap and lying in the acoustic-optical region), showing that these systems have a clear phonon frequency gap in the  $[001]$  direction. A perusal of the panels in Fig. 1 clearly shows that, as one would expect, increasing the mismatch between the two materials of a superlattice, both in terms of force constants and masses, increases the size of the polarization gaps and hence increases the size of the clear phonon frequency gap in the  $[001]$  direction. The largest contributing factor for

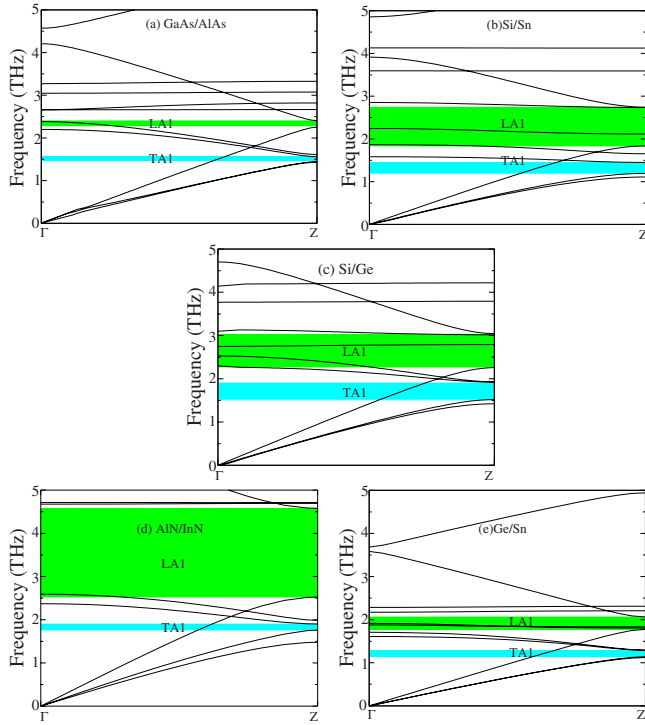


FIG. 1. (Color online) Phonon dispersion curves for (a)  $(\text{GaAs})_2(\text{AlAs})_2[001]$ , (b)  $(\text{Si})_2(\text{Sn})_2[001]$ , (c)  $(\text{Si})_2(\text{Ge})_2[001]$ , (d)  $(\text{AlN})_2(\text{InN})_2[001]$ , and (e)  $(\text{Ge})_2(\text{Sn})_2[001]$  superlattices along the growth direction. Only the acoustic range is shown and the lowest acoustic gaps (LA1 and TA1) are indicated.

increasing the gap size is the mass difference between the two constituent materials forming the superlattice, with the force constant changes being less important. This is highlighted from the results for the three IV/IV superlattices where the mass ratios  $m(\text{Si}):m(\text{Ge}):m(\text{Sn})$  are 1.0:2.7:4.2 and the difference in the force constants is smaller than 15%.

In addition to (2,2) superlattices, we also made calculations for other larger superlattices. Two important results of note are the (23,9) GaAs/AlAs superlattice recently designed and studied by Lanzillotti-Kimura *et al.*<sup>40</sup> and the  $\text{Si}(4 \text{ nm})/\text{Si}_{0.4}\text{Ge}_{0.6}(8 \text{ nm})[001]$  superlattice fabricated and studied by Ezzahri *et al.*<sup>19</sup> For the (23,9) GaAs/AlAs superlattice, we have identified TA-TA gaps centered 0.176, 0.375, and 0.56 THz, and LA-LA gaps at 0.265 and 0.54 THz. The LA-LA gap centered 0.54 THz ( $18 \text{ cm}^{-1}$ ) occurs at the Brillouin zone center and can be compared well with the results presented by Lanzillotti-Kimura *et al.*<sup>40</sup> using a continuum theory and Raman measurements. For the  $\text{Si}(4 \text{ nm})/\text{Si}_{0.4}\text{Ge}_{0.6}(8 \text{ nm})[001]$  superlattice, three LA-LA gaps identified at 0.25, 0.50, and 0.81 THz agree with the results presented by Ezzahri *et al.* We have previously shown that this superlattice is a true one-dimensional phononic.<sup>30</sup>

It is important to note that when one considers changing phonon wavevector from the [001] growth direction to another direction, say the [100] direction, these gaps eventually close, leading to continuous frequency spectra and thus a finite total density of states. This means that when considering the full three-dimensional density of states, the frequency spectrum is continuous. However, in the [001] direction, there will be a depletion in the number of states available at

TABLE II. The positions of the gaps, their sizes, and the panel reference to Fig. 1 for the five  $(\text{A})_2/(\text{B})_2[001]$  superlattices.

Superlattice	Gap position (THz)	Gap size (THz)	Panel in Fig. 1
GaAs/AlAs	2.34	0.1	(a)
Si/Sn	1.99	0.2	(b)
Si/Sn	2.49	0.5	(b)
Si/Ge	2.64	0.2	(c)
Si/Ge	2.91	0.2	(c)
AlN/InN	3.58	2.0	(d)
Ge/Sn	1.99	0.1	(e)

certain energies due to the gaps that have been opened up. These gaps would thus contribute to directional anisotropy in phonon related thermal properties (Table II).

The phonon dispersion of the  $\text{Si}_2/\text{Ge}_2[001]$  superlattice presented in Fig. 1(b) has been studied previously by several groups.<sup>41</sup> As can be seen when one compares our results in Fig. 1(b) with the work by Gironcoli<sup>11</sup> using a force constant *ab initio* approach, there is exceptionally good agreement between the two. Similarly there is clear agreement between the results presented in Fig. 1(a) and the results obtained by Ren *et al.*<sup>13</sup> for the  $\text{GaAs}_2/\text{AlAs}_2[001]$  superlattice using the rigid ion model. This and other results which are also in agreement<sup>14,42</sup> lends credence to the EBCM approach adopted here and hence shows that the dispersion curves for the other superlattices presented can be expected to be accurate. However, while the previous works did not examine the one-dimensional phononic properties of superlattices, in the present work we will now present a comprehensive study of both the variation in the stop bands as a function of length fraction and period, and also the role of interface mixing on these bands.

## B. Predicting one-dimensional phononic gaps

To understand how to predict clear one-dimensional phononic gaps in the frequency spectra of superlattices, one needs to examine the variation in the locations of the individual LA and TA gaps with both layer thickness and length fraction. In Fig. 2 we demonstrate a method for finding the location of one-dimensional phononic gaps in solid systems, using GaAs/AlAs as an example. This figure presents the variation in the locations of these gaps with the layer thickness for the  $(\text{GaAs})_n(\text{AlAs})_n[001]$  superlattices. Above 1 THz, the TA4 and LA2 polarization gaps coincide and a shared gap occurs at 2.36 THz for the (4,4) superlattice, and the TA4 and LA3 gaps coincide resulting in a shared gap at 1.69 THz for the (8,8) superlattice. For the (16,16) superlattice two one-dimensional gaps occur above 1 THz: the first at 1.39 THz (where the TA8 and LA5 gaps coincide) and the second at 1.69 THz (where the TA10 and LA6 gaps coincide). In the subterahertz region (below 1 THz) one-dimensional phononic gaps of quite small size occur for the  $(n,n)$  superlattices with  $n \geq 8$ . These features are highlighted with the regions shaded in the golden color. In particular, the lowest gap occurs for  $n \sim 20$  with  $L_f = 0.5$  at  $\sim 0.45$  THz, where the TA3 and LA2 gaps cross over. As these results



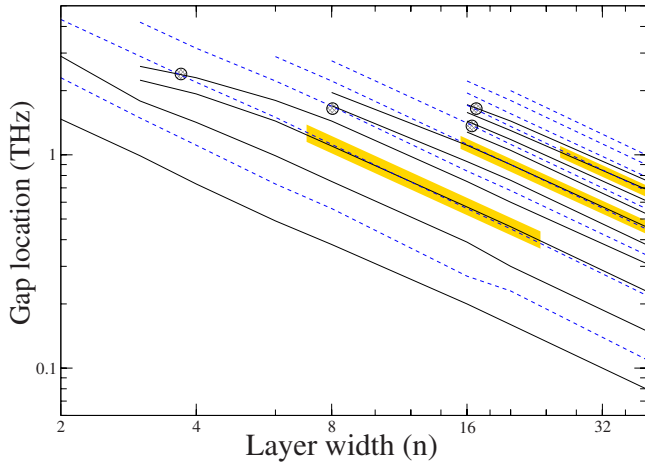


FIG. 2. (Color online) Variation in a few LA and TA gap locations with the layer thickness index  $n$  in  $(\text{GaAs})_n(\text{AlAs})_n[001]$  superlattices. Highlighted in gold are the regions with phononic gaps and specific phononic gaps are shown with dots.

vary as  $1/L_0$  (as can be clearly seen from Fig. 2) and additional gaps open up for larger and larger superlattices, we expect that one-dimensional phononic gaps for all sizes of superlattices will be found.

For larger systems, the creation of additional phononic gaps is not simple to predict. However, there exists a simple method to estimate the location of the gaps that are produced for very large superlattices without the need for additional calculations. By locating a gap in a thin superlattice, it is apparent that each time one doubles the period, a new gap will be created at the same frequency as the first gap. This is because the doubling of the superlattice period manifests as the Brillouin zone being folded onto itself. Thus the gaps in the LA and TA folded branches at the Brillouin zone edge for a certain superlattice period will be found at the zone center with the same frequencies when the period doubles. For example, on the basis of the results presented in Fig. 2 for the (8,8), (16,16), and (32,32) superlattices, we can predict a one-dimensional phononic gap at approximately 0.9 THz for the (64,64) GaAs/AlAs superlattice, and we have confirmed this result with further direct calculations. This method, based on the combination of accurate results for thinner samples and the zone-folding technique, can be applied to predict polarization gaps in any thick  $(A)_n(B)_n$  superlattice and should help future calculations and experiments to search for more accurate results.

The second parameter we consider when discussing polarization gaps in superlattices is the length fraction  $L_f$  of material B in the A/B superlattice. We present a technique similar to that applied earlier for differing periods, but focus on the length fraction parameter. To continue to show the applicability of the technique to all superlattices, we use Si/Ge for our example this time. Figure 3 shows the variation in the positions of several LA and TA polarization gaps as a function of  $L_f$  for  $(\text{Si})_n(\text{Ge})_m[001]$  superlattices of the fixed period  $L_0$ , with  $n+m=20$  (for the case  $n=m=10$ ,  $L_0=11.08$  nm). It is clearly seen that as the percentage of germanium increases the positions of the polarization gaps decrease. As can also be seen from the figure, the second LA

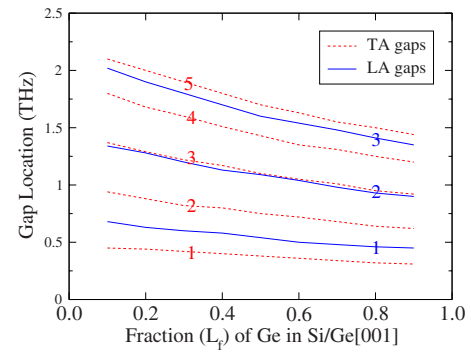


FIG. 3. (Color online) Variation in gap locations with Ge length fraction  $L_f$  for various  $(\text{Si})_n(\text{Ge})_m[001]$  superlattices with  $n+m=20$ . For each polarization, the  $i$ th gap is indicated on the figure.

gap and the third TA gap coincide for the entire range of the percentage of germanium considered. These two lines can be described with an approximately linear fit within a small error margin. From the results for the period dependence of  $(n,n)$  superlattices and using the linear fit from Fig. 3, the prediction of this one-dimensional gap to arise in Si/Ge[100] superlattices can be made with the following empirical formula:

$$\nu_{\text{gap}} = (-0.563L_f + 1.406)\frac{\bar{L}}{L}, \quad (1)$$

where  $\nu_{\text{gap}}$  is the frequency in terahertz of the center of the gap,  $L$  is the superlattice period in nanometers,  $L_f$  is the length fraction of germanium in silicon within the range 0.1–0.9, and  $\bar{L}=5.54$  nm. However, it should be pointed out that this relation is an approximation as at large values of  $L$  the gaps become too small to be detectable. Also, as the period increases the widths of the LA and TA gaps may become smaller than the difference between the locations of the two gaps. For integer multiples of  $\bar{L}$ , other gaps can be predicted from this formula as discussed previously. Furthermore, this technique should be readily applicable to all superlattices.

### C. Role of interface mixing and defects

Superlattices in reality do not have ideal interfaces, but instead a slight degree of mixing at the interface is expected.<sup>43–46</sup> This mixing may also change the in-plane periodicity.<sup>12,47</sup> These effects are expected to change electronic, vibrational, and thermal properties of the system. From the point of view of vibrational and phonon-related properties the dominant effect can be expected to arise from the mass intermixing across the interface. We will show here that the mixing has less effect on the phononic properties than might be simply guessed.

First, we point out that in the Si/SiGe superlattices grown by Ezzahri *et al.*<sup>19</sup> the  $\text{Si}_{0.4}\text{Ge}_{0.6}$  layer can assume several different possible atomic configurations within the unit cell. In our previous work<sup>30</sup> consideration of different atomic make-up for the  $\text{Si}_{0.4}\text{Ge}_{0.6}$  layer was found to shift the frequencies by only approximately 0.06 THz for modes in the low acoustic region (less than 1 THz). Since for phononic systems the main focus is in the region of 2.5 THz and be-

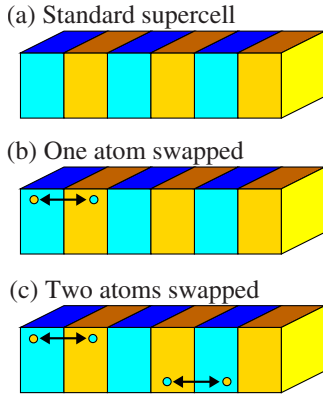


FIG. 4. (Color online) A schematic illustration of the supercell for: (a) a  $3 \times (A)_n(B)_n$  superlattice, (b) a  $3 \times (A)_n(B)_n$  superlattice with one defect introduced, and (c) a  $3 \times (A)_n(B)_n$  superlattice with two defects introduced.

low, we confirm that mass mixing within a layer does not change the essential gap property of Si/SiGe superlattices.

Second, in Fig. 4 we present a schematic of three supercells which we have modeled to examine the role of defects

in superlattices. These consist of (a) the pure supercell, (b) the same cell with one defect, and (c) the same cell again with two defects. Figures. 5–7 show the phonon dispersion relations for these unit cells for Si/Ge and GaAs/AlAs superlattices with the introduction of defects in the form of interdiffusion of atoms across interfaces. In particular, we have considered an enlarged supercell consisting of three (8,8) bilayer superlattice subcells for Si/Ge and three (4,4) bilayer superlattice subcells for GaAs/AlAs. Such considerations are also illustrative of what is observed for larger unit cell configurations. However, much larger unit cell configurations are not presented here as the additional zone folding that occurs due to the longer period produces phonon dispersion curves with a much larger number of branches which prove difficult to present in a manner that is clear and concise.

Figure 5 shows the phonon dispersion results, for various superlattices with different defects, in the first terahertz region (i.e., in the frequency range 0–1 THz). As can be seen, even introducing quite a large amount of disorder into these systems has not changed the results significantly. The picture

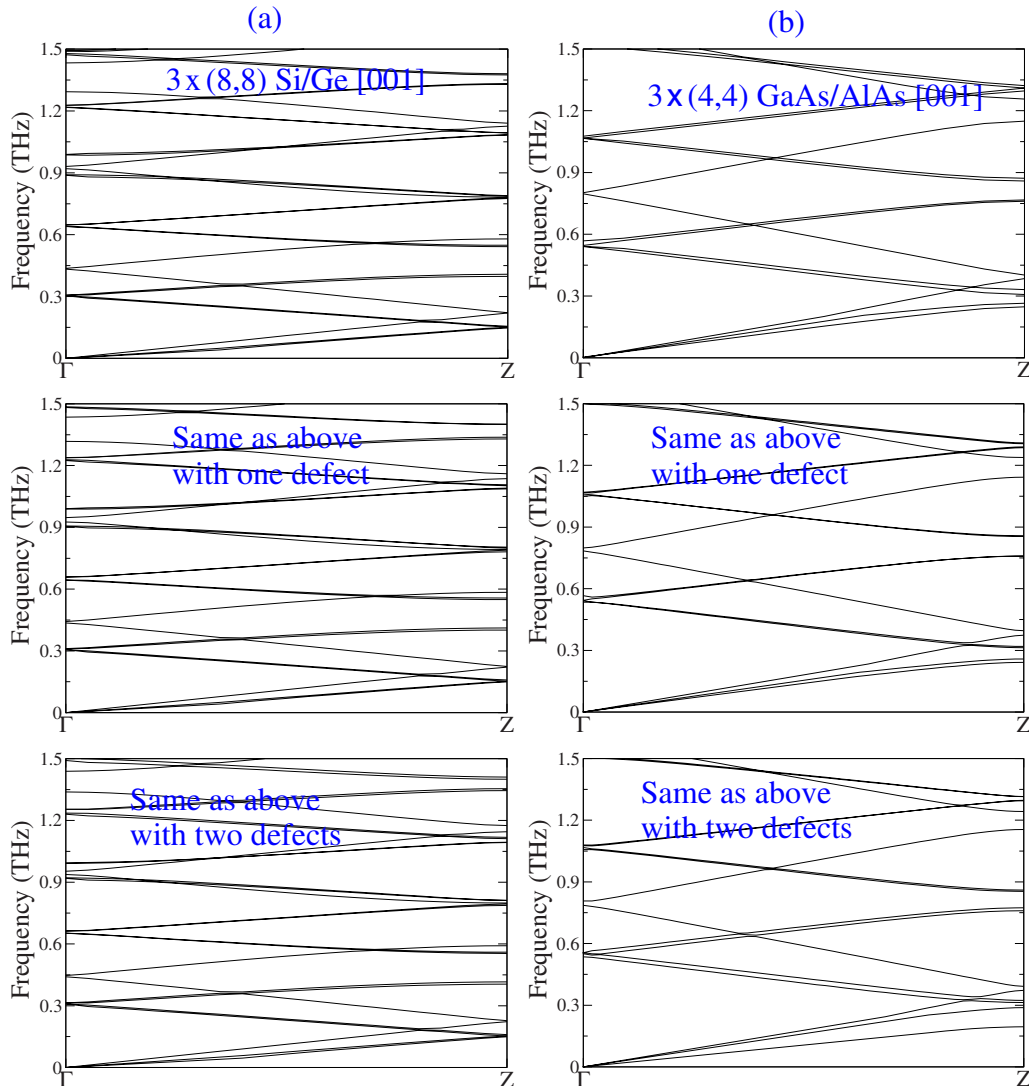


FIG. 5. (Color online) The phonon dispersion curves in the low acoustic range of: (a) the  $3 \times (\text{Si})_8(\text{Ge})_8$  superlattice and (b) the  $3 \times (\text{GaAs})_4(\text{AlAs})_4$  superlattice. To assess the role of mass defects, results are presented with zero, one, and two atomic swaps as illustrate in Fig. 4. The  $3 \times$  means three repeat unit cells of the A/B superlattice, i.e., the supercell consists of A/B/A/B/A/B.

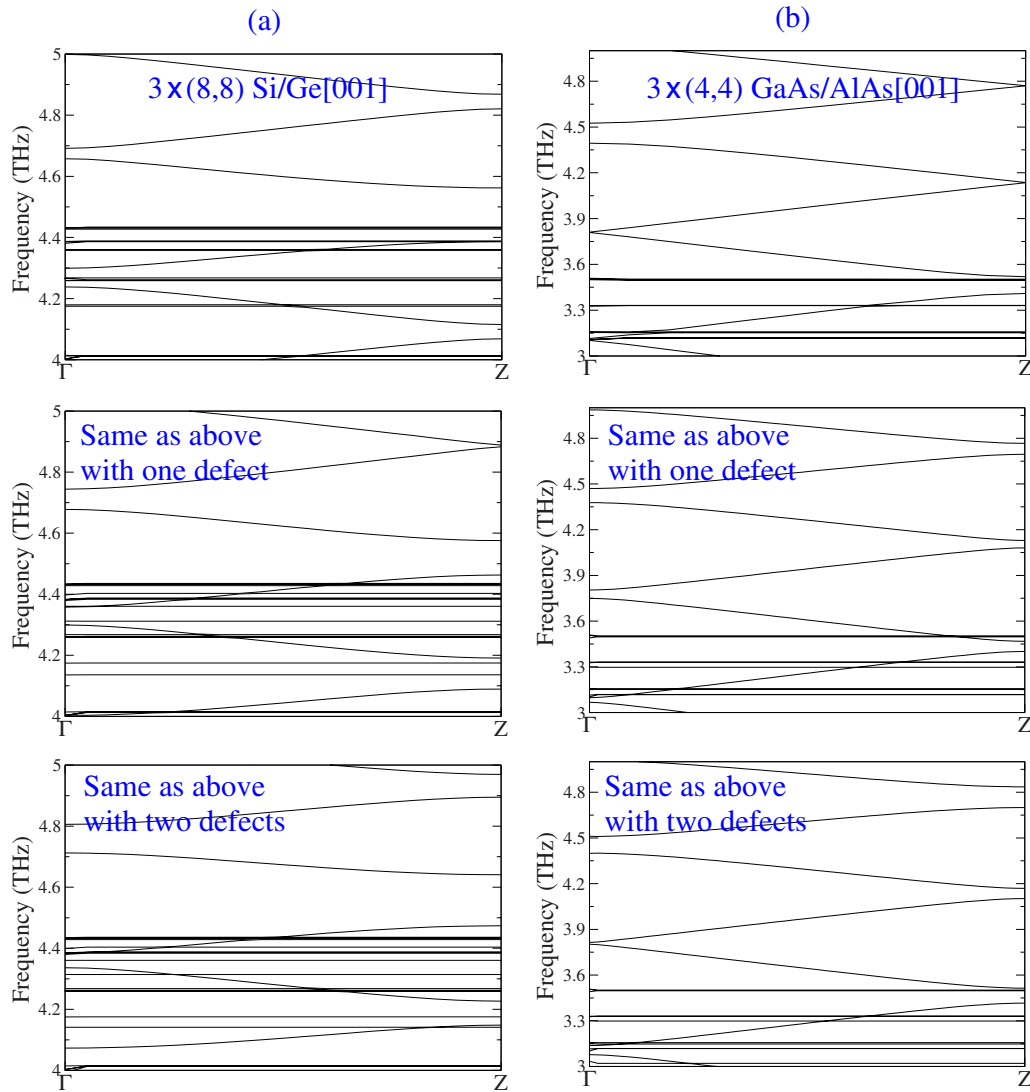


FIG. 6. (Color online) Same as in Fig. 5, but showing the midfrequency range.

is the same in the range 1–2.5 THz with a shift of less than 0.05 THz in the phonon dispersion relations. Conversely, at the high optical frequencies, the flattened optical modes are often said to be *confined* or localized to the individual material layers, due to the superlattice structure. As can be seen from Fig. 7 the introduction of impurities increases the spread of the bands of these modes, which can be simply described as being due to either increasing or decreasing the width of the individual layers that the optical phonon modes are localized in. However, these modes still maintain near zero velocity due to the localization. Also, as can be seen from the figures, the introduction of defects does not lead to a decrease in the position of the highest optical modes, which is to be expected as this is a property of the overall system and less dependent on local phenomena. The behavior of this mode with superlattice period has been predicted by Jusserand *et al.*<sup>16</sup> and our results here show that this behavior does not appear to change with the introduction of a small amount of interface mixing.

The region which the introduction of defects has the greatest effect is the mid-frequency region (approximately 4–6 THz) as seen in Fig. 6. In this region the shift can be of

the order of 0.3 THz, but nevertheless, the polarization gaps remain. Again, we limit our discussion to under these frequencies where the tuning of the properties is more possible. It is worth noting that at the higher frequencies the gaps created are still present as expected. However, the presence of defects has shifted these modes. On the other hand, from the point of view of engineering phononic systems, and clearly highlighted by Fig. 6, while the presence of defects does create additional gaps, it does not close existing ones. This can be expected and is not surprising, as the breaking of the original periodicity leads to band splitting in general.

Interfaces in superlattices are potential scatterers of heat carrying phonons (i.e., these alter the phonon lifetime). A system with a sharp interface can be considered as the unperturbed superlattice system and its phonon spectrum can be modeled as described in Secs. III A and III B. However, a system with an intermixed interface is characterized by defects which will scatter phonons of the unperturbed system and thus contribute to the phonon scattering rate. Such a scattering rate is better described using time dependent perturbation theory. The small shifts and gaps in the phonon spectrum of the systems with defects presented above lend

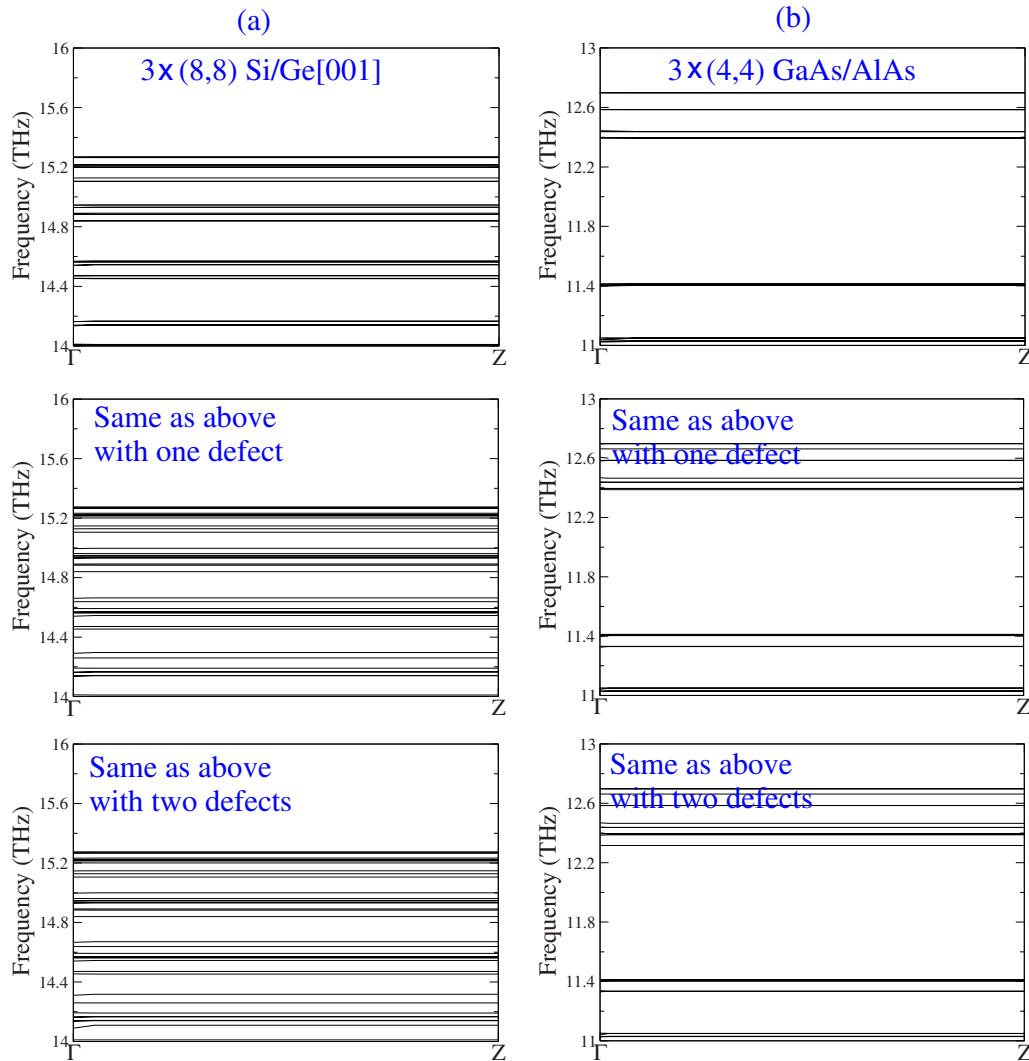


FIG. 7. (Color online) Same as Fig. 5, but showing the optical range.

support to this approach. Our discussion further suggests that while there are difficulties in growing smooth interfaces on the nanoscale, the tuning of phonon related properties of such systems is possible. This is especially true of thermal properties of a nanophononic system, which are essentially governed by the phonon acoustic branches.

#### D. One-dimensional versus three-dimensional phononic crystals

It is pertinent to discuss why studying one- or two-dimensional phononics is just as important as their three-dimensional counterparts which show an absolute stop band, or forbidden zone. First, the subject of phononics draws a lot of analogies from photonics. In photonics, two-dimensional and one-dimensional gaps are routinely discussed despite having propagating modes in the second and third dimensions.<sup>48,49</sup>

The second reason is as follows. Three-dimensional and one-dimensional phononics both present several interesting properties depending on the design of the system. It is possible to produce one- and two-dimensional phononic crystals with large vibrational anisotropy. In view of this, one would expect thermal properties of the system to also present great

anisotropy due to the changes in the phonon velocities and the phonon density of states. Using Fig. 8, we illustrate how this anisotropy arises for one-dimensional phononic crystals. Generally, the density of states for bulk at a frequency  $\omega$  is

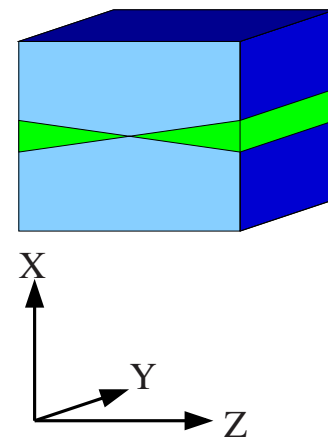


FIG. 8. (Color online) An schematic illustration of allowed (blue) and disallowed (green) states at a given frequency as a function of wavevector within the Brillouin zone for a one-dimensional phononic crystal. The Z-direction is the growth direction and the center of the cube represents the zone center, the  $\Gamma$  point.



contributed by states from wavevectors in all directions. In contrast, for a one-dimensional phononic crystal, with the frequency gap at  $\omega$ , there are no modes available in the  $\Gamma$ -Z direction. This has two effects: (i) the total density of states at the frequency  $\omega$  is reduced when compared to the bulk system, and (ii) at frequency  $\omega$  the density of states is anisotropic. Hence, this means that the resulting thermal properties, such as heat transport, are anisotropic, with a minimum in the [001] direction.

As illustrated in Fig. 8, while there are no states available for phonon wavevectors strictly along [001], adding any other component to the wavevector may make states at this frequency available and hence will contribute to the thermal properties in the [001] direction. This, however, is still true when one compares with three-dimensional phononic systems as the modes with lower energies also possess this feature and hence will contribute to thermal transport in the [001] direction. Thus, the engineering of one-dimensional phononic crystals is expected to provide much more interesting phonon physics than systems with complete gaps existing in all three dimensions.

#### IV. SUMMARY

In summary, we have provided a methodology for predicting phononic gaps in thin semiconductor superlattices. First we have shown that several different choices of ultra thin superlattices possess one-dimensional phononic gaps and that the greater the difference between each layer's vibrational properties the greater the size of the gaps. The  $(\text{Si})_n(\text{Ge})_m[001]$  and  $(\text{GaAs})_n(\text{AlAs})_m[001]$  superlattices are found to be one-dimensional phononic crystals, with similar results expected for other semiconducting superlattices. We have also shown that the gap positions in both these structures vary inversely with the superlattice period and have presented a method for predicting gap locations in thicker structures once these are found in thin structures.

Quantitative predictions have been made for the positions of the LA and TA gaps with the Ge length fraction  $L_f$  in  $(\text{Si})_n(\text{Ge})_m$  superlattices for the period given by  $n+m=20$ , and for GaAs/AlAs structures with differing periods and  $L_f=0.5$ . It has been shown that the technique can be applied to any superlattice. Furthermore, an empirical formula has been provided for the location of a one-dimensional phononic gap in Si/Ge[001] superlattices for different length fractions and periods. Again, it is pointed out that such a relation could be easily found for other superlattices.

Our work suggests that the effect of interface mixing rarely leads to the closure of phononic gaps. We have shown that the introduction of mass defects has the greatest effect for the high acoustic range in shifting frequencies, but does not close any pre-existing phononic gaps. We have also confirmed the expected result that defects broaden bands in the optical range.

Finally, we have discussed the important merits and implications of one-dimensional phononic systems when compared to their three-dimensional counterparts. We believe

that these results would prove useful to both experimentalists and theorists in understanding vibrational and thermal properties of semiconductor superlattices.

#### ACKNOWLEDGMENTS

S.H gratefully acknowledges financial support from the Leverhulme Trust. The calculations reported here were performed using the University of Exeter's SGI Altix ICE 8200 supercomputer.

- <sup>1</sup>S. M. Lee, D. G. Cahill, and R. Venkatasubramanian, *Appl. Phys. Lett.* **70**, 2957 (1997).
- <sup>2</sup>W. S. Capinski, H. J. Maris, T. Ruf, M. Cardona, K. Ploog, and D. S. Katzer, *Phys. Rev. B* **59**, 8105 (1999).
- <sup>3</sup>J.-C. Hsu and T.-T. Wu, *Phys. Rev. B* **74**, 144303 (2006).
- <sup>4</sup>Z. G. Wang, S. H. Lee, C. K. Kim, C. M. Park, K. Nahm, and S. A. Nikitov, *J. Phys.: Condens. Matter* **20**, 055209 (2008).
- <sup>5</sup>T. Gorishnyy, C. K. Ullal, M. Maldovan, G. Fytas, and E. L. Thomas, *Phys. Rev. Lett.* **94**, 115501 (2005).
- <sup>6</sup>J.-F. Robillard, A. Devos, and I. Roch-Jeune, *Phys. Rev. B* **76**, 092301 (2007).
- <sup>7</sup>J. O. Vasseur, P. A. Deymier, B. Djafari-Rouhani, Y. Pennec, and A.-C. Hladky-Hennion, *Phys. Rev. B* **77**, 085415 (2008).
- <sup>8</sup>S. Yang, J. H. Page, Zhengyou Liu, M. L. Cowan, C. T. Chan, and P. Sheng, *Phys. Rev. Lett.* **93**, 024301 (2004).
- <sup>9</sup>S. T. Huxtable and A. R. Abramson, C.-L. Tien, A. Majumdar, C. LaBounty, X. Fan, G. Fan, G. Zeng, J. E. Bowers, A. Shakouri, and E. T. Croke, *Appl. Phys. Lett.* **80**, 1737 (2002).
- <sup>10</sup>G. H. Zeng, J. E. Bowers, J. M. O. Zide, A. C. Gossard, W. Kim, S. Singer, A. Majumdar, R. Singh, Z. Bian, Y. Zhang, and A. Shakouri, *Appl. Phys. Lett.* **88**, 113502 (2006).
- <sup>11</sup>S. de Gironcoli, *Phys. Rev. B* **46**, 2412 (1992).
- <sup>12</sup>E. Molinari, S. Baroni, P. Giannozzi, and S. de Gironcoli, *Phys. Rev. B* **45**, 4280 (1992).
- <sup>13</sup>S.-F. Ren, H. Chu, and Y.-C. Chang, *Phys. Rev. B* **37**, 8899 (1987).
- <sup>14</sup>Z. Jian, Z. Kaimung, and X. Xide, *Phys. Rev. B* **41**, 12862 (1990).
- <sup>15</sup>L. D. Landau and E. M. Lifshitz, *Theory of Elasticity* (Butterworth-Hienemann, Washington, DC, 1988).
- <sup>16</sup>H. Jusserand, D. Paquet, and A. Regreny, *Phys. Rev. B* **30**, 6245 (1984).
- <sup>17</sup>A. K. Sood, J. Menéndez, M. Cardona, and K. Ploog, *Phys. Rev. Lett.* **54**, 2111 (1985).
- <sup>18</sup>B. Jusserand, D. Paquet, F. Mollot, F. Alexandre, and G. Le Roux, *Phys. Rev. B* **35**, 2808 (1987).
- <sup>19</sup>Y. Ezzahri, S. Grauby, J. M. Rampnoux, H. Michel, G. Pernot, W. Claeys, S. Dilhaire, C. Rossignol, G. Zeng, and A. Shakouri, *Phys. Rev. B* **75**, 195309 (2007).
- <sup>20</sup>M. S. Kushwaha, P. Halevi, G. Martinez, L. Dobrzynski, and B. Djafari-Rouhani, *Phys. Rev. B* **49**, 2313 (1994).
- <sup>21</sup>M. S. Kushwaha, *Int. J. Mod. Phys. B* **10**, 977 (1996).
- <sup>22</sup>M. S. Kushwaha, *Recent Res. Dev. Appl. Phys.* **2**, 743 (1999).
- <sup>23</sup>M. Sigalas, M. S. Kushwaha, E. N. Economou, M. Kafesaki, I. E. Psarobas, and W. Steurer, *Z. Kristallogr.* **220**, 765 (2005).
- <sup>24</sup>F. Herman, *J. Phys. Chem. Solids* **8**, 405 (1959).
- <sup>25</sup>A. A. Maradudin, E. W. Montroll, G. H. Weiss, and I. P. Ipatova, *Theory of Lattice Dynamics in the Harmonic Approximation*, 2nd ed. (Academic, New York, 1971).
- <sup>26</sup>W. Kress, H. Borik, and R. Wehner, *Phys. Status Solidi B* **29**, 133 (1968).
- <sup>27</sup>J. S. Jensen, *J. Sound Vibrat.* **266**, 1053 (2003).
- <sup>28</sup>P. G. Martinsson and A. B. Movchan, *Q. J. Mech. Appl. Math.* **56**, 45 (2003).
- <sup>29</sup>A. Huynh, N. D. Lanzillotti-Kimura, B. Jusserand, B. Perrin, A. Fainstein, M. F. Pascual-Winter, E. Peronne, and A. Lemaître, *Phys. Rev. Lett.* **97**, 115502 (2006).
- <sup>30</sup>S. P. Hepplestone and G. P. Srivastava, *Phys. Rev. Lett.* **101**, 105502 (2008).
- <sup>31</sup>W. Weber, *Phys. Rev. B* **15**, 4789 (1977); K. C. Rustagi and W. Weber, *Solid State Commun.* **18**, 673 (1976).
- <sup>32</sup>H. M. Tütüncü and G. P. Srivastava, *Phys. Rev. B* **62**, 5028 (2000).
- <sup>33</sup>H. M. Tütüncü, G. P. Srivastava, and S. Duman, *Physica B* **316–317**, 190 (2002).

- <sup>34</sup>H. M. Tütüncü and G. P. Srivastava, *J. Phys.: Condens. Matter* **8**, 1345 (1996).
- <sup>35</sup>P. Keating, *Phys. Rev.* **145**, 637 (1966).
- <sup>36</sup>W. J. Brya, *Solid State Commun.* **12**, 253 (1973).
- <sup>37</sup>A. T. Khan, P. R. Berger, F. J. Guarin, and S. S. Iyer, *Appl. Phys. Lett.* **68**, 3105 (1996).
- <sup>38</sup>H. A. Calderón, M. A. Vidal, and H. Ladrón de Guevara, *Microscopy and Microanalysis* **12**, 712 (2006).
- <sup>39</sup>T. Fujii, K. Shimomoto, R. Ohba, Y. Toyoshima, K. Horiba, J. Ohta, H. Fujioka, M. Oshima, S. Ueda, H. Yoshikawa, and K. Kobayashi, *Appl. Phys. Express* **2**, 011002 (2009).
- <sup>40</sup>N. D. Lanzillotti-Kimura, A. Fainstein, A. Lemaitre, and B. Jusserand, *Appl. Phys. Lett.* **88**, 083113 (2006).
- <sup>41</sup>R. A. Ghanbari, J. D. White, G. Fasol, C. J. Gibbings, and C. G. Tuppen, *Phys. Rev. B* **42**, 7033 (1990).
- <sup>42</sup>E. Molinari and A. Fasolino, *Appl. Phys. Lett.* **54**, 1220 (1989).
- <sup>43</sup>K.-Q. Chen, X.-H. Wang, and B.-Y. Gu, *Phys. Rev. B* **62**, 9919 (2000).
- <sup>44</sup>K.-Q. Chen, X.-H. Wang, and B.-Y. Gu, *Phys. Rev. B* **65**, 153305 (2002).
- <sup>45</sup>A. V. Kosobutski and E. N. Malysheva, *Semiconductors* **42**, 1208 (2008).
- <sup>46</sup>W. Braun, L. Däweritz, and K. H. Ploog, *Phys. Rev. B* **55**, 1689 (1997).
- <sup>47</sup>D. Berdekas and S. Ves, *J. Phys.: Condens. Matter* **21**, 275405 (2009).
- <sup>48</sup>S. C. Kitson, W. L. Barnes, and J. R. Sambles, *Phys. Rev. Lett.* **77**, 2670 (1996).
- <sup>49</sup>T. Rindzevicius, Y. Alaverdyan, M. Kall, W. A. Murray, and W. L. Barnes, *J. Phys. Chem. C* **111**, 11803 (2007).